Catalysis Communications 170 (2022) 106502

Contents lists available at ScienceDirect

Catalysis Communications

journal homepage: www.elsevier.com/locate/catcom

Experimental investigation of anion exchange membrane water electrolysis for a tubular microbial electrosynthesis cell design

Zhiyuan Chen, Asier Grijalvo Rodriguez, Pello Nunez, Diane van Houtven, Deepak Pant *, Jan Vaes

Separation & Conversion Technology, Flemish Institute for Technological Research (VITO), Boeretang 200, Mol 2400, Belgium

ARTICLE INFO

Keywords:
Hydrogen
Pressurized reactor
Membrane electrode assembly
Tubular electrode

ABSTRACT

Tubular water splitting electrolyzer was adapted to neutral pH conditions for the in-situ H_2 supplying microbial electrosynthesis design. The electrolyzer was optimized to reduce ohmic losses and provide adequate gas separation. Direct membrane deposition was applied on a thin anionic exchange membrane for the membrane-electrode-assembly fabrication. Although the membrane resistance increased with the increasing membrane thickness from 55 to 165 μm, the contact resistance was reduced by applying stronger compression pressure on the membrane-electrode interface. A durability test was run for 120 h, showing a voltage increase of 134 μV/h. Moreover, the hydrogen permeability coefficient was determined at 10^{-14} mol/(m·s·Pa).

1. Introduction

Microbial electrosynthesis (MES) is an effective way to convert CO_2 to valuable multi-carbon reduced end-products [1]. Microbial species use hydrogen and CO_2 to generate products, acetate for instance, in the reactor. Hydrogen evolution reaction (HER) is deemed as the most promising pathway to provide a key intermediate element, hydrogen, to the industrial up-scaled microbial CO_2 reduction process [2]. In this case, the process contains two parts: water electrolysis (WE) and microbial reduction [3,4]. It is known that oxygen and hydrogen are produced as the anodic and cathodic products in water electrolysis. To separate oxygen from the anaerobic cathodic environment, a polymer electrolyte membrane or composite membrane is needed in this reactor. A polymer electrolyte membrane water electrolysis part of the bioreactor will be studied and optimized in this work.

The membrane electrode assembly (MEA) is the core part of a MES or the WE sub-system. MEA contains a polymer electrolyte membrane which has close contact with an anode and a cathode on the two sides of it. The membrane is usually Nafion® for proton-conduction. An anion exchange membrane (AEM) is an alternative material for the electrolyte. The employment of AEM results in a high pH of the system and thus can substitute non-platinum-group-metal as the electrode and reduce the corrosion issues of the other components. As one of the promising AEMs, the Aemion™ membrane [5] was employed in this work. Hydroxyl (OH^-) ions are produced in the water reduction and migrate through AEM towards the anode. At the anode, OH^- is oxidized to produce oxygen and electrons.

This work describes the WE sub-system as a tubular cell, which was designed as a container for microbial species. The membrane is direct membrane deposited (DMD) [6] on the microporous anode tube, and a catalyst coated membrane (CCM) is applied for the cathode fabrication. As the purpose of the cell is designed for MES, it is not safe to use KOH aqueous solution as an electrolyte for electrochemical reactions. Thus demineralized water is employed in this work for the study of HER. A low current density and high overpotential can be expected for the AEM electrolyzer working with pure water. Ito et al. [7] indicated that the cell voltage (U_{cell}) reached 2.2 V at a current density (i) of 0.1 A/cm^2 with an unstable cell resistance of 1.4 Ω cm^2 at 50 °C. It is equal to 104 mL/min H_2 production rate in the under-study reactor. However, the reported hydrogen generation rates in a MES reactors were even slower than this value. The typical values are 45.6 ± 18.8 μM/min [8] (<1.44 mL/min H_2 for the under-study reactor), 48.0 ± 1.5 μmol/h/cm^2 [9] (<2.77 mL/min H_2 for the under-study reactor), and 10 L/m^2/day [10] (0.104 mL/min H_2 for the under-study reactor) in the recent reports. It indicates that improvement of the electrochemical performance of WE tubular cells in the MES reactor is much required.

The microbial electrochemical reduction rate of CO_2 is not only related to the HER kinetics but also the gas permeability. Permeation of gases through the membrane is a critical safety issue in the WE sub-system. Hydrogen crossover through the membrane causes the loss of

* Corresponding author.
E-mail address: deepak.pant@vito.be (D. Pant).

https://doi.org/10.1016/j.catcom.2022.106502
Received 29 June 2022; Received in revised form 12 August 2022; Accepted 1 September 2022
Available online 5 September 2022

hydrogen and also contaminates the oxygen product. It is a safety risk and an energy unnecessary consumption. Oxygen crossover can break the anoxic environment in the catholyte and results in the inactivation of microbial species. It is known that hydrogen permeability through the membrane is higher than that of oxygen [7,11], therefore the crossover of hydrogen was measured for the characterization of gas permeability.

2. Materials and experiments

A zero-gap tubular cell is fabricated for the in-situ H_2 supplying microbial electrosynthesis (Fig. 1s) and the water electrolysis experiments in this system are reported in this work. A porous Ni 200 tube with an outer diameter of 14 mm and a length of 450 mm is employed as the anode (Fig. 1). The average pore size in the tube is 0.2 μm. Aminion® high IEC anion exchange polymer (AP1-HNN8–00-X) is cast on the Ni tube as an anode supported AEM. The ionomer solution is prepared by dissolving 10 wt% of ionomer in methanol. The DMD approach is manufactured with three different membrane thicknesses (55 μm for Cell-1, 88 μm for Cell-2, and 165 μm for Cell-3) and is compared with the state-of-the-art membrane (AF1-HNN8–50-X, 50 μm for Cell-0). The thickness of the membrane is calculated from the mass of the ionomer solution and referred to as the status before swelling in water.

Carbon with 10 wt% Pt loading is prepared as ink to be directly deposited on the casted AEM to form a CCM on the cathode side. The Pt loading on the cathode is 0.2 mg/cm^2. The catalyst ink for the casting is prepared with 0.8 g Pt/C catalyst powders, 1.6 mL ionomer solution, and 28 mL 2-propanol. Nickel felt is used as the cathode porous transport layer (PTL) for the cathode.

The reactor is designed with a containing volume of 1 L. Four tubular cells can be built inside it to separate cathodic and anodic chambers (Fig. 1). In this work, for the proof of concept, only one tubular cell is measured as a batch mode in the experiments. Demineralized water is fed into the anode side and cathode side for electrochemical testing.

Electrochemical measurements are performed with a Biologic potentiostat (VMP3) and a booster at room temperature. U_{cell} is measured at each level of current (I) with chronopotentiometry. For each measurement, I was increased to a certain value and kept for a certain time to reach a stable value of U_{cell}. The electrolyzer was also characterized by electrochemical impedance spectroscopy (EIS). The high-frequency resistance (HFR) at high frequencies (usually >1 kHz) is obtained from the spectrum as the state-of-health and degradation monitoring of the electrolyzer [12]. The low-frequency resistance (LFR) intercept from the EIS spectrum is also recorded at around 1 Hz. The EIS is flowing a polarization at the same cell voltage for 3 min.

For safety considerations, the gas crossover is measured in the reactor. There are several methods to measure the reactant crossover through the membrane in the electrolyzer. Hydrogen crossover through the fuel cell membrane was tested with the leakage current method [13] and pressurized method [14] in this work. For the first method, the anode side is kept at ambient pressure (1 atm). The pressure difference between the open anode and the sealed cathode was measured with a pressure transmitter. A small current was applied to the electrolyzer, which produces hydrogen and oxygen on the two sides of the membrane, and the pressure of the cathode side reached a steady state, when the electrochemical hydrogen evolution is compensated by the hydrogen crossover, $G_{H_2}^{loss}$:

$$G_{H_2}^{loss} = \frac{I}{2AF} \tag{1}$$

where, I is the current of the electrolyzer, A is the active area of the membrane, and F is the Faraday constant. It is easy to follow that the $G_{H_2}^{loss}$ does not only include the crossover of hydrogen but also the leakage of hydrogen through the sealing points in the reactor. Oxygen crossover is ignored here because of its low permeability compared to hydrogen [15] and the relatively high pressure of the cathode suppresses oxygen crossover. Hydrogen permeation rate, k_{H_2}, can be converted from the measured hydrogen crossover flux:

$$k_{H_2} = G_{H_2}^{loss} \frac{t}{\Delta p_{H_2}} \tag{2}$$

where, t is the measuring time, Δp_{H_2} is the pressure difference. The second method can be employed as an in-situ technology with measuring the mass transfer limited current for hydrogen permeation. The cyclic voltammetry (CV) technique was used in this work for the measurement. A scan rate of 2 mV s^{-1} was applied and the limiting current region between the potential range between 400 and 600 mV was extracted for the calculation:

$$k_{H_2} = \frac{1}{2F} \frac{d}{p_{H_2}} \left(\frac{I}{A} - \frac{V_{cell}}{R_s A} \right) \tag{3}$$

where, d is the thickness of the membrane, V_{cell} is the measured cell voltage, R_s is the estimated electrical short resistance. The value of R_s is inversely proportional to the electrical short current in the limited current region.

The stability of the cell is tested by a moderate constant current hold at 2.5 A for 120 h without draining or refilling the electrolyte in the reactor.

3. Results and discussion

3.1. Performance

The performance of the electrolyzer was characterized by i-U_{cell}

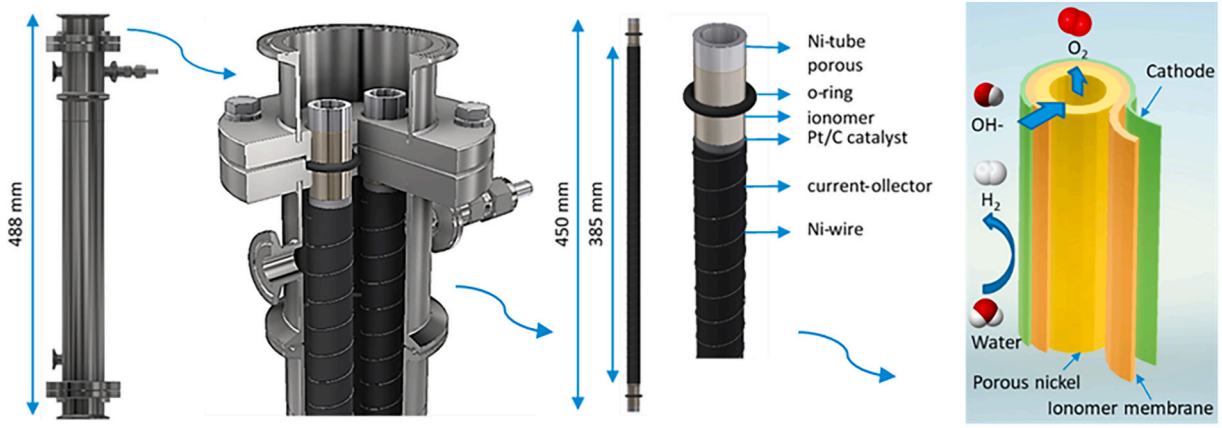

Fig. 1. Reaction scheme of a tubular cell and reactor design.

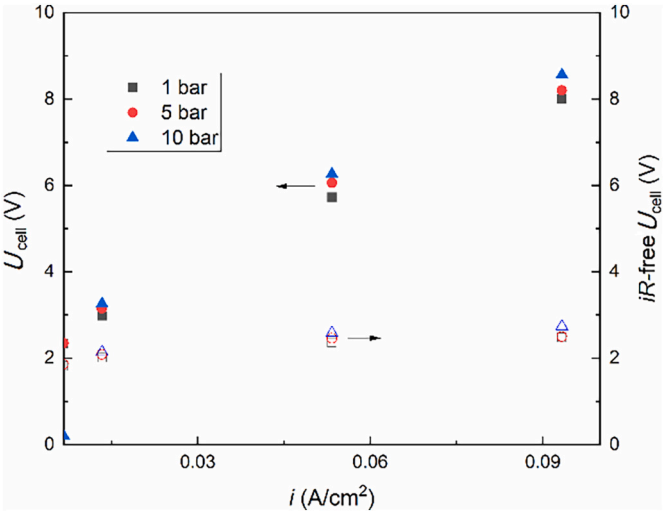

Fig. 2. Cell voltage (U_{cell}) and *iR*-free cell voltage (*iR*-free U_{cell}) of Cell-0 versus current density with demineralized water as the electrolytic solution at room temperature under different pressures.

(Fig. 2) under different pressures in the range of up to 10 bar. The pressures of the cathode and anode are balanced in the measurement. The high cell voltage of the electrolyzer in Fig. 2 is mostly attributed to the large ohmic loss. The *iR*-free U_{cell} was also calculated by subtracting the ohmic losses from the cell voltage. Fig. 2 shows that, under 1 bar, the U_{cell} is 8.01 V at the current density of 0.93 A/cm^2, but the corresponding *iR*-free U_{cell} is equal to 2.48 V. Accordingly, a high value of HFR is shown in Fig. 3.

According to the Nernst equation, the thermodynamic cell voltage increases as a function of pressure at a limited value [16]. Both the two cell voltage values show a weak increase with the increase of balanced pressure. Correspondingly, the values of HFR and LFR only show small differences in the applied pressure range (Fig. 3). It indicates that the measurement under 1 atm is presentative for the electrochemical performance measurement of the electrolyzer. As shown in Fig. 3, HFR is independent of the current density, but LFR decreases with increasing current density. The value of LFR-HFR is corresponding to the cathodic and anodic processes. Fig. 3 shows that the charge transfer resistance decreases strongly by nearly two orders of magnitude with the increasing current density and cell voltage. The anodic process is usually slower than the cathodic process. Therefore, it mostly contributed to the oxygen evolution reaction overpotential.

The value of HFR at 0.93 A/cm^2 is 56.6 Ω cm^2, and the corresponding value of LFR is 59.3 Ω cm^2. The relatively small difference between LFR and HFR values at 0.93 A/cm^2 indicates ohmic loss is the principal reason for the high overpotential in the electrolysis. The improvement of the cell performance needs an efficient reduction of the cell ohmic resistance, which includes the membrane resistance, material resistance of the components, and contact resistances. The membrane resistance can be adjusted by changing the membrane thickness, and the contact resistance is affected by the assembly technologies of the cell, including the MEA fabrication and the current contact between the MEA and the current collector. The material resistance matters in tubular cell configuration because of its unique current flow. Different from a planar cell, current flow through the circumferential cross-section of the Ni tube and PTL to one of the ends of the cell, reaching the current collector. It is obvious that the length of the cell has a negative effect on the ohmic loss in the current collection [17]. As a result, the ohmic loss in the electrode is larger than that in a planar cell with the same materials.

In order to improve the membrane resistance and contact resistance, the membrane with different thicknesses was fabricated by DMD. Compared to the state-of-art membrane, the method of DMD improves

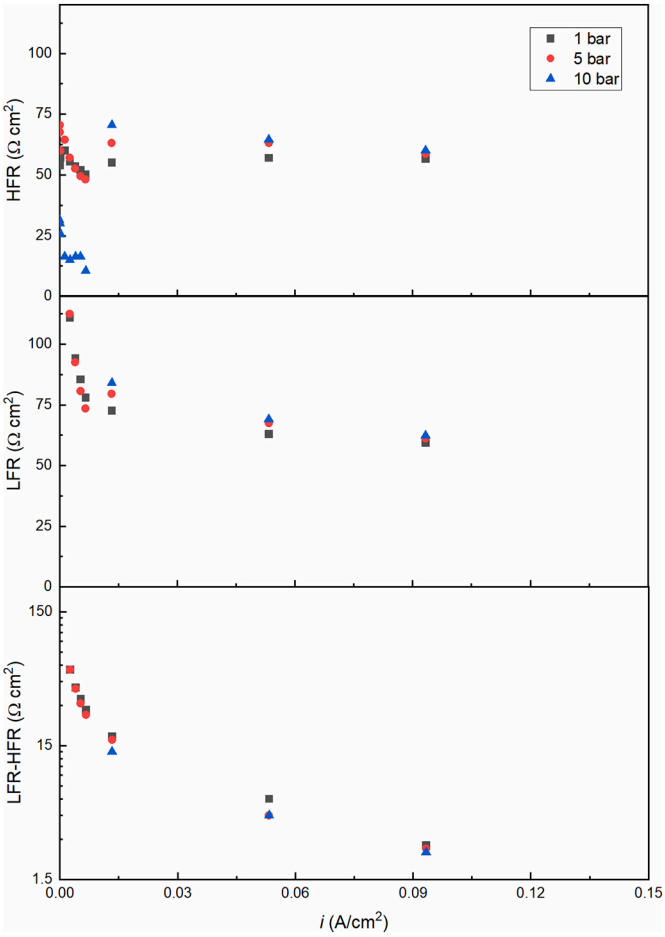

Fig. 3. High-frequency resistance (HFR), low-frequency resistance (LFR), and the value of LFR-HFR of Cell-0 versus current density with demineralized water as the electrolytic solution at room temperature under different pressures.

the overall electrochemical performance significantly (Fig. 4). The U_{cell} and *iR*-free U_{cell} are 3.0 V and 2.3 V, respectively. The corresponding HFR and LFR are 7.1 and 8.31 Ω cm^2, respectively. Fig. 5 shows that the HFR can decrease by 55% to 88% from its original value in Fig. 3. It can be the result of improved interface contact between the Ni tube and the

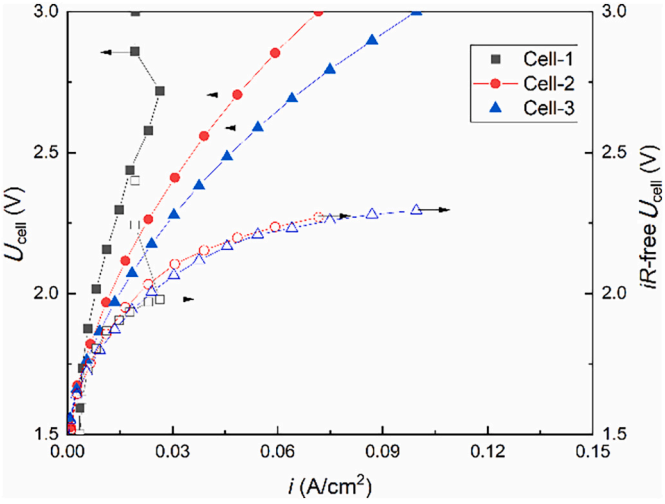

Fig. 4. Cell voltage (U_{cell}) and *iR*-free cell voltage (*iR*-free U_{cell}) of cells versus current density with demineralized water as the electrolytic solution at room temperature under 1 atm.

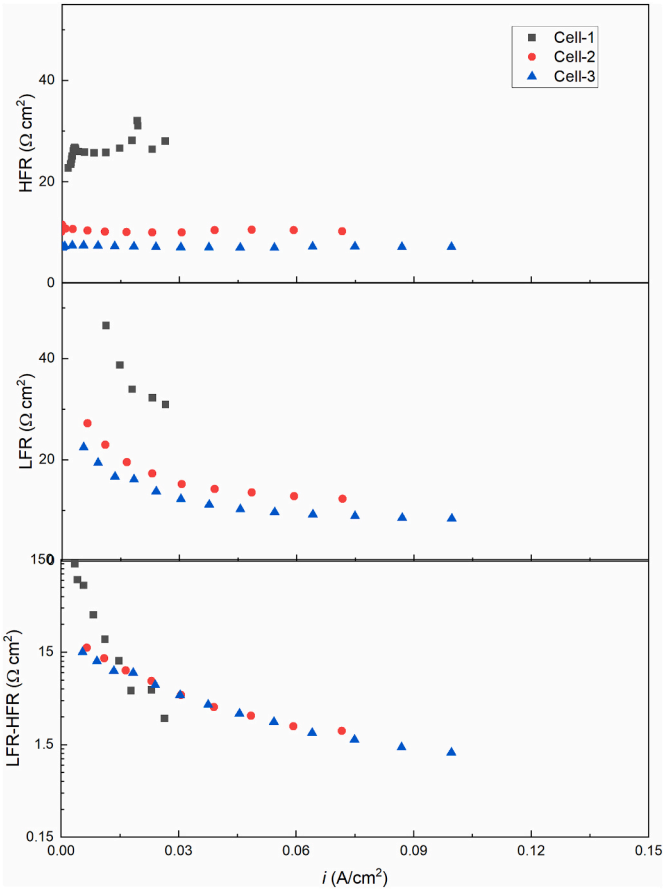

Fig. 5. (a) High-frequency resistance (HFR), (b) low-frequency resistance (LFR), and (c) the value of LFR-HFR of cells versus current density with demineralized water as the electrolytic solution at room temperature under 1 atm.

membrane. A slightly decreased value of LFR-HFR in Fig. 5 implies that the improving contact in the MEA could also have some positive influence on the anodic kinetics. Photos of the MEA before and after electrolysis are shown in Fig. 6 as a comparison of the status of the MEA with the state-of-art membrane and DMD membrane. Fig. 6 shows that the state-of-art membrane swells along the tube direction, generating folds periodically. It is because that the metallic wires fix the PTL tightly on the MEA, and the force between the wires is weaker than that under the wires. Whilst, the DMD membrane contacts the porous Ni tube firmly which restricts swelling in the area.

Usually, it should be expected that the cell with a thinner membrane shows a better electrochemical performance. It is well-known that the area-specific resistance (ASR) of a membrane is equal to the thickness/ion conductivity. Therefore, theoretically, the membrane resistance increases linearly with the membrane thickness. The measured ASR of the AF1-HNN8–50 membrane is 1.74 ± 0.28 Ω cm^2 in 0.5 M NaCl solution [18]. The same material with a thickness of 165 μm could increase to 5.74 Ω cm^2 under identical conditions. Experimentally, Holzapfel et al. [6] showed that such improvement is accounted for the decrease of HFR for a thin membrane. The study of Fortin et al. [5] on the same type of membrane as used in this work also indicates that the reduced membrane thickness results in a lower membrane ohmic resistance and thus overall better cell performance. However, this was not the case in the present study. An obvious better electrochemical performance of the electrolyzer and lower HFR value was observed for the membrane with higher thickness. It implies that the contribution of membrane resistance to the total ohmic loss can be ignored, and the declined HFR with a thick membrane could also be the result of reduced contact resistance. A high thickness can improve the mechanical stability of the membrane, and then suppress the strip-off between the membrane and Ni tube. As long as the membrane and electrode contacting well, swelling in the thickness direction promote the clamping force between the wire on the PTL and the porous Ni tube. This force is stronger when the membrane is thicker. The increased compression force could lower the contact resistance thus improve the electrochemical performance of the electrolyzer [19,20].

It should be noted that, with the modification of detailed operation steps in the fabrication of MEA, either for the state-of-art membrane or employing DMD technology, the ohmic loss can be optimized. It is also mostly contributed to the suppressing of contact resistance. The contact resistance can also be strongly influenced by the selection of PTL materials and the compressing method of PTL on the MEA. The trails in Fig. 2s show that the improvement of PTL lowers the value of HFR. Other than membrane resistance and contact resistance, the material resistance of the components is also important for tubular cells. Bipolar plates with large cross-section areas are used for the electric connection for planar cells, thus the material resistance of them can be very small. However, only wires/belts with a limited cross-section area can be used for the tubular cell. Moreover, the selection of electrical wires needs to consider corrosion resistance and biocompatibility thus limiting the composition of materials. Here stainless steel wires were chosen as the electrical wires, of which the conductivity is significantly lower than copper and silver. Therefore, the ohmic resistance of the electrical wires is the principal component of the HFR. A shortened wire can

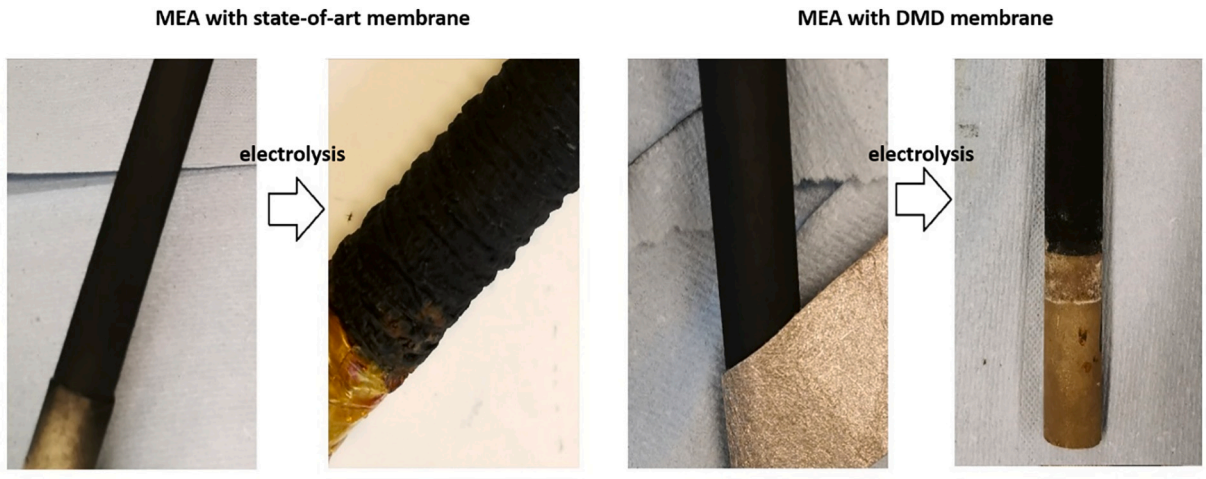

Fig. 6. Morphology of two different MEAs before electrolysis and after electrolysis.

significantly reduce the HFR of the cell.

The voltage evolution of the cell-3 was tested at a constant current hold at 2.5 A, which is the current that would be applied for the upcoming reaction in the reactor, for 120 h (Fig. 7). The voltage increased by 134 μV/h on average. This degradation rate is slightly lower than the reported values [21,22], due to the more moderate current density in this work compared to the literature. However, long-term electrolysis still needs to be tested.

3.2. Hydrogen crossover

It can be noted that the thinner membrane has a high hydrogen crossover rate. Therefore, the membrane with 55 μm thickness is employed for the hydrogen cross-over measurement to make sure the system can even work with the thinnest membrane. Two techniques were employed for the determination of the hydrogen crossover through the membrane in this work. Pressure difference at the two sides of the membrane was built for both of the two methods, thus it can be expected that the hydrogen crossover test results also partly indicate the gas tightness of the reactor.

3.2.1. Pressurized method

Stepwise current densities were applied within the range between 167 μA/cm^2 and 500 μA/cm^2. The corresponding stable cathode pressure increased with the current and the range is from 0.15 bar to 0.22 bar. The hydrogen permeability coefficient was calculated with Eqs. (1) and (2), and the results are shown in Fig. 3s. The permeability values are from 8.0 × 10^{-14} to 18.0 × 10^{-14} mol/(m s Pa). The value at low cathodic pressures ($\leq$ 0.19 bar) is of the same order of magnitude as the literature data [13]. However, an increase in hydrogen permeability with pressure was observed at high pressure. It could be due to the O-ring at the end of the tubular cell could not keep gas tightness with the high-pressure difference between the two electrode chambers.

3.2.2. Leakage current method

The potential range between 330 and 530 mV is selected for the evaluation of hydrogen crossover, where the current linearly changes with the applied cell voltage (Fig. 4s). The value of R_s can be estimated from the slope of the fitting line. The values of parameters for the evaluation of hydrogen crossover are listed as follows: $p_{H_2} = 0.02$ bar, $A = 150$ cm^2, $U_{cell}/R_s = 6.10 \times 10^{-3}$ mA/cm^2. The thickness change of the Aemion™ membrane was reported to be around 21% [23], d is estimated as 67 μm. Although this method is sensitive to variations of operation parameters [13], the measurement result shows a reliable value of the k as 8.0 × 10^{-14} mol/(m s Pa), which is similar to the value obtained from the pressurized method. Both the results with the two methods indicate that the hydrogen permeability can be well controlled within a reasonable range in the test.

4. Conclusions

The electrochemical water electrolysis performance of a tubular cell with an anion exchange membrane was investigated under a demineralized water environment in a batch reactor mode at room temperature. The ohmic loss (high-frequency resistance) was optimized in this work. It was found that contact resistance has a high impact on ohmic loss. The development of MEA with direct membrane deposition improved the contact between Ni tube and membrane, thus improving the performance of the electrolyzer. The cell voltage is improved to be 3.0 V at 0.1 A/cm^2 in demineralized water at room temperature with a deposited membrane thickness of 155 μm. The increase of membrane thickness can lower the value of HFR efficiently by raising compressing pressure in the MEA. The contact resistance in MEA can be efficiently reduced by applying such pressure. A safety measurement was carried out for the electrolyzer. The hydrogen permeability coefficient is at 10^{-14} mol/(m s Pa) below the cathodic pressure of 0.20 bar for the cell with a membrane thickness of 55 μm. It indicates that this tubular cell can be integrated into a MES system without destroying the anoxic bacterial growth environment.

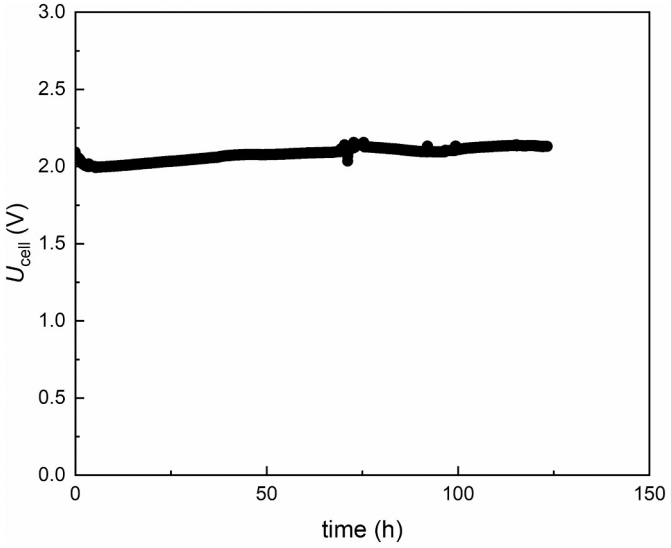

Fig. 7. Voltage evolution during a total constant current hold at 2.5 A of cell-3.

CRediT authorship contribution statement

Zhiyuan Chen: Conceptualization, Methodology, Formal analysis, Investigation, Writing – original draft, Visualization, Data curation. **Asier Grijalvo Rodriguez:** Investigation. **Pello Nunez:** Investigation. **Diane van Houtven:** Resources, Methodology, Investigation. **Deepak Pant:** Conceptualization, Resources, Methodology, Writing – review & editing, Funding acquisition. **Jan Vaes:** Resources, Supervision, Writing – review & editing.

Declaration of Competing Interest

Deepak Pant reports financial support was provided by the European Commission.

Acknowledgement

This project has received funding from the European Union's Horizon 2020 research and innovation programme under grant agreement No 82599 (Bac-To-Fuel).

Appendix A. Supplementary data

Supplementary data to this article can be found online at https://doi.org/10.1016/j.catcom.2022.106502.

References

[1] D.R. Lovley, K.P. Nevin, Electrobiocommodities: powering microbial production of fuels and commodity chemicals from carbon dioxide with electricity, Curr. Opin. Biotechnol. 24 (3) (2013) 385.
[2] X. Ma, G. Zhang, F. Li, M. Jiao, S. Yao, Z. Chen, Z. Liu, Y. Zhang, M. Lv, L. Liu, Boosting the microbial Electrosynthesis of acetate from CO_2 by hydrogen evolution catalysts of Pt nanoparticles/rGO, Catal. Lett. 151 (10) (2021) 2939.
[3] E. Blanchet, F. Duquenne, Y. Rafrafi, L. Etcheverry, B. Erable, A. Bergel, Importance of the hydrogen route in up-scaling electrosynthesis for microbial CO_2 reduction, Energy Environ. Sci. 8 (12) (2015) 3731.
[4] S. Tian, H. Wang, Z. Dong, Y. Yang, H. Yuan, Q. Huang, T.-s. Song, J. Xie, Mo_2 C-induced hydrogen production enhances microbial electrosynthesis of acetate from CO_2 reduction, Biotechnology for Biofuels 12 (1) (2019) 1.
[5] P. Fortin, T. Khoza, X. Cao, S.Y. Martinsen, A. Oyarce Barnett, S. Holdcroft, High-performance alkaline water electrolysis using Aemion™ anion exchange membranes, J. Power Sources 451 (2020), 227814.

[6] P. Holzapfel, M. Bühler, C. Van Pham, F. Hegge, T. Böhm, D. McLaughlin, M. Breitwieser, S. Thiele, Directly coated membrane electrode assemblies for proton exchange membrane water electrolysis, Electrochem. Commun. 110 (2020), 106640.
[7] H. Ito, N. Kawaguchi, S. Someya, T. Munakata, N. Miyazaki, M. Ishida, A. Nakano, Experimental investigation of electrolytic solution for anion exchange membrane water electrolysis, Int. J. Hydrogen Energy 43 (36) (2018) 17030.
[8] E. Perona-Vico, L. Feliu-Paradeda, S. Puig, L. Bañeras, Bacteria coated cathodes as an in-situ hydrogen evolving platform for microbial electrosynthesis, Sci. Rep. 10 (1) (2020) 19852.
[9] F. Kracke, A.B. Wong, K. Maegaard, J.S. Deutzmann, M.A. Hubert, C. Hahn, T. F. Jaramillo, A.M. Spormann, Robust and biocompatible catalysts for efficient hydrogen-driven microbial electrosynthesis, Commun. Chem. 2 (1) (2019) 45.
[10] S.S. Lim, B.H. Kim, D. Li, Y. Feng, W.R.W. Daud, K. Scott, E.H. Yu, Effects of applied potential and reactants to hydrogen-producing biocathode in a microbial electrolysis cell, Frontiers in Chemistry 6 (2018) 318.
[11] H. Ito, T. Maeda, A. Nakano, H. Takenaka, Properties of Nafion membranes under PEM water electrolysis conditions, Int. J. Hydrogen Energy 36 (17) (2011) 10527.
[12] T. Lin, L. Hu, W. Wisely, X. Gu, J. Cai, S. Litster, L.B. Kara, Prediction of high frequency resistance in polymer electrolyte membrane fuel cells using long short term memory based model, Energy and AI 3 (2021), 100045.
[13] M. Schoemaker, U. Misz, P. Beckhaus, A. Heinzel, Evaluation of hydrogen crossover through fuel cell membranes, Fuel Cells 14 (3) (2014) 412.
[14] B. Bensmann, R. Hanke-Rauschenbach, K. Sundmacher, In-situ measurement of hydrogen crossover in polymer electrolyte membrane water electrolysis, Int. J. Hydrogen Energy 39 (1) (2014) 49.
[15] K. Broka, P. Ekdunge, Oxygen and hydrogen permeation properties and water uptake of Nafion® 117 membrane and recast film for PEM fuel cell, J. Appl. Electrochem. 27 (2) (1997) 117.
[16] M. Suermann, A. Pătru, T.J. Schmidt, F.N. Büchi, High pressure polymer electrolyte water electrolysis: Test bench development and electrochemical analysis, Int. J. Hydrogen Energy 42 (17) (2017) 12076.
[17] A.V. Virkar, F.F. Lange, M.A. Homel, A simple analysis of current collection in tubular solid oxide fuel cells, J. Power Sources 195 (15) (2010) 4816.
[18] A.S. Gangrade, S. Cassegrain, P. Chandra Ghosh, S. Holdcroft, Permselectivity of ionene-based, Aemion® anion exchange membranes, J. Membr. Sci. 641 (119917) (2022).
[19] D. Henkensmeier, M. Najibah, C. Harms, J. Žitka, J. Hnát, K. Bouzek, Overview: state-of-the art commercial membranes for anion exchange membrane water electrolysis, J. Electrochem. Energy Convers. Storagee 18 (2) (2020) 024001.
[20] S.H. Frensch, A.C. Olesen, S.S. Araya, S.K. Kær, Model-supported characterization of a PEM water electrolysis cell for the effect of compression, Electrochim. Acta 263 (2018) 228.
[21] C. Klose, T. Saatkamp, A. Münchinger, L. Bohn, G. Titvinidze, M. Breitwieser, K. D. Kreuer, S. Vierrath, All-hydrocarbon MEA for PEM water electrolysis combining low hydrogen crossover and high efficiency, Adv. Energy Mater. 10 (14) (2020) 1903995.
[22] A.R. Motz, D. Li, A. Keane, L.D. Manriquez, E.J. Park, S. Maurya, H. Chung, C. Fujimoto, J. Jeon, M.K. Pagels, C. Bae, K.E. Ayers, Y.S. Kim, Performance and durability of anion exchange membrane water electrolyzers using down-selected polymer electrolytes, J. Mater. Chem. A 9 (39) (2021) 22670.
[23] B. Shanahan, B. Britton, A. Belletti, S. Vierrath, M. Breitwieser, Performance and stability comparison of Aemion™ and Aemion+™ membranes for vanadium redox flow batteries, RSC Adv. 11 (22) (2021) 13077.